

Thermal analysis of organically modified Ca²⁺-montmorillonite using DSC and TSC techniques

N. A. Halim¹ · Aidy Ali²  · Z. H. Z. Abidin³ · A. B. Ahmad³ · A. Z. Sulaiman¹ · Z. A. Ibrahim²

Received: 9 June 2016 / Accepted: 6 November 2016 / Published online: 14 November 2016
© Akadémiai Kiadó, Budapest, Hungary 2016

Abstract Thermal analysis on organically modified Ca²⁺-montmorillonite (OMON) and its source materials—octadecylamine (ODA) and Ca²⁺-montmorillonite (Ca²⁺-Mon)—was studied using thermally stimulated current (TSC) technique. The appearance of ρ_{MON} peak with the $T_{\text{max}} = 75$ °C shows the ability of the developed TSC system to demonstrate the relaxation effects of dehydration in Ca²⁺-Mon. It appeared within the temperature range of DSC endothermic peak (30–100 °C) where the $T_{\text{mMON}} = 58$ °C. Segmental motions of ODA chains and structural disruptions in the modifier agent compound produced TSC α_{ODA} , ρ_{ODA} and $\rho_{1\text{ODA}}$ peaks that are comparable to thermal transition and endothermic peaks in DSC profile (T_{gODA} , T_{m1ODA} and T_{m2ODA}). The effect of localized motion in ODA chains as revealed by the TSC β_{OMON} peak ($T_{\text{max}} = -23$ °C), however, is absent in the DSC profile of OMON. It shows TSC technique has high sensitivity in detecting various relaxation behaviors at molecular level. More evidences are demonstrated by the ρ_{OMON} ($T_{\text{max}} = 86$ °C) and $\rho_{1\text{OMON}}$ ($T_{\text{max}} = 105$ °C) peak originated from the ODA chains structures. These peaks also confirm the intercalation of the modifier cations inside the Ca²⁺-Mon gallery.

Keywords Ca²⁺-montmorillonite · Modifier molecule · TSC · DSC · XRD and intercalation

Introduction

Large amount of exchangeable cations inside montmorillonite layers generate a peculiar hydration giving swelling property that explains the extensive interlayer expansion of the clay minerals. The ability to swell makes the clay useful for many applications such as in oil industry, agriculture, pharmaceutical and fabrication of polymer composites [1–4]. The highly charged surface and exchangeable cations in pristine montmorillonite (MON), however, make the clay interaction with nonpolar polymers difficult. Therefore, chemical modification by exchanging the clay counterion for organocation is necessary in order to transform its property from organophobic into organophilic.

Chemical modification normally involved the intercalation of modifier molecules such as alkyl ammonium cation into the montmorillonite gallery. In our previous work [5], we had shown the presence of modifier molecules inside the clay gallery of organically modified montmorillonite (OMON) was hardly detected using the differential scanning calorimetry (DSC) technique. A more sensitive technique thus is needed to detect the effect of confined space of the clay gallery on molecular motions.

TSC technique was employed to investigate the molecular motions within polymeric materials [6, 7]. The thermoelectrical technique is a dielectric spectroscopy method to study the electrical properties of high-resistivity solids, through their thermal relaxation effects [8–10]. In TSC technique, current induced by thermal increase from an electret is measured with a definite heating scheme. The

✉ Aidy Ali
saidynaidy@gmail.com

¹ Center for Defence Foundation Studies, Universiti Pertahanan Nasional Malaysia (UPNM), Kem Sg. Besi, 57000 Kuala Lumpur, Malaysia

² Department of Mechanical Engineering, Faculty of Engineering, Universiti Pertahanan Nasional Malaysia (UPNM), Kem Sg. Besi, 57000 Kuala Lumpur, Malaysia

³ Department of Physics, University of Malaya, 50603 Kuala Lumpur, Malaysia

current is generated by the buildup and release of polarized charge carriers inside the solid dielectrics sandwiched between two electrodes. TSC technique enjoys attention due to its capability to resolve complex dielectric relaxations within low equivalent frequency, $f \sim 10^{-1} - 10^{-4}$ Hz [8]. The high sensitivity thus makes the TSC technique useful to study primary and secondary relaxation in many amorphous or semicrystalline dielectric materials.

In this present work, a laboratory-scale TSC system was used to investigate the thermoelectrical property of solid dielectrics. Thermal analysis by means of both TSC and DSC techniques were undertaken on Ca^{2+} -montmorillonite, octadecylamine and OMON.

The beauty of this study, the attempt is made on correlating the TSC and DSC peak. Analysis revealed that the good sensitivity of TSC technique not just makes it a comparable method to the DSC, but it is capable of demonstrating the thermoelectrical behaviors of intercalated organic molecules inside Ca^{2+} -montmorillonite gallery.

Experimental

Materials

Ca^{2+} -montmorillonite SWy2 (Ca^{2+} -Mon) was supplied by the University of Missouri, USA, from the Clay Mineral Society Repository in Wyoming. The chemical formula of Ca^{2+} -Mon can be expressed as $\text{Ca}^{2+}-(\text{Al}, \text{Mg})_2\text{Si}_4\text{O}_{10}(\text{OH})_2 \cdot n\text{H}_2\text{O}$. The amount of exchangeable cation in between the Ca^{2+} -Mon layers is represented by the cation exchange capacity, CEC of about 76.4 meq/100 g. Octadecylamine (ODA) ($\geq 99\%$) and hydrochloride acid (HCl, 4.0 M in H_2O), used in organoclay modification, were purchased from Fluka (Malaysia). All the materials were used as received without further purification.

Sample preparation

Organically modified Ca^{2+} -montmorillonite (OMON)

Eight grams of pristine Ca^{2+} -Mon clay mineral was dispersed into 500 mL of distilled water at a temperature of about 80 °C using a homogenizer. A total of 3.1 g of ODA was dissolved in 200 mL of distilled water (80 °C) together with 1.2 mL of concentrated HCl. The mixture was then gradually poured into the Ca^{2+} -Mon-water solution under vigorous stirring for 5 min. The white precipitate obtained was then collected on a white cloth filter and washed using distilled water (80 °C) five times. The organophylic Ca^{2+} -Mon (OMON) precipitate finally was allowed to dry at ambient temperature [11].

Characterization

X-ray diffraction, XRD

The X-ray diffraction, XRD, measurement was performed using Siemens XRD diffractometer model D5000. A nickel-filtered $\text{Cu K}\alpha$ radiation ($\lambda = 0.154$ nm) was employed with the applied voltage of 40 kV and a current of 40 mA. The XRD patterns were recorded with a step size of 0.02° from $2\theta = 2^\circ$ to $2\theta = 50^\circ$. The changes in basal spacing, d , of the Ca^{2+} -Mon particles were determined by analyzing the XRD data, which was carried out based on the Bragg's law [12].

$$n\lambda = 2d \sin \theta \quad (1)$$

where n = an integer, k = constant (generally = 0.9) m, λ = wavelength (0.1541 nm), d = basal spacing (nm), and θ = the diffraction angle ($^\circ$).

Differential scanning calorimetry, DSC

The Rheometric Scientific DSC Gold with a heat flux system was used for the differential scanning calorimetry (DSC) measurement. The measurement was performed on samples at the heating rate of $10^\circ\text{C min}^{-1}$, after quenching the temperature down to -100°C using liquid nitrogen. Thermal responses from the scans were recorded at temperature ranging from -100 to 200°C . The sample mass used was 8.0 mg.

Thermally stimulated current, TSC

TSC measurements were performed with a TSC system developed in the laboratory [11]. In this work, TSC samples were press-molded into disk shape where the contact area is 127.5 mm^2 and thickness of about 0.8 mm. A pair of metal electrode held the TSC sample in a cryostat. Samples were subjected to an electric field F_p for a polarization time, t_p , at a polarization temperature T_p . Polarized dipoles and charges were then frozen by quenching the sample temperature to a T_o . At this temperature, the electrical field F_p was removed and sample temperature stabilized for t_s minutes. The electret sample was then short-circuited and heated at a constant rate, 1°C min^{-1} . As a result, the discharge current, I , was generated by the depolarization process of electret charges. The current density J_D from TSC measurements is given by [13]

$$J_D(T) = \frac{P_e(T_p)}{\tau_o} \exp\left(-\frac{E}{kT}\right) \exp\left[-\frac{1}{h\tau_o} \int_{T_o}^T \exp\left(-\frac{E}{kT'}\right) dT'\right] \quad (2)$$

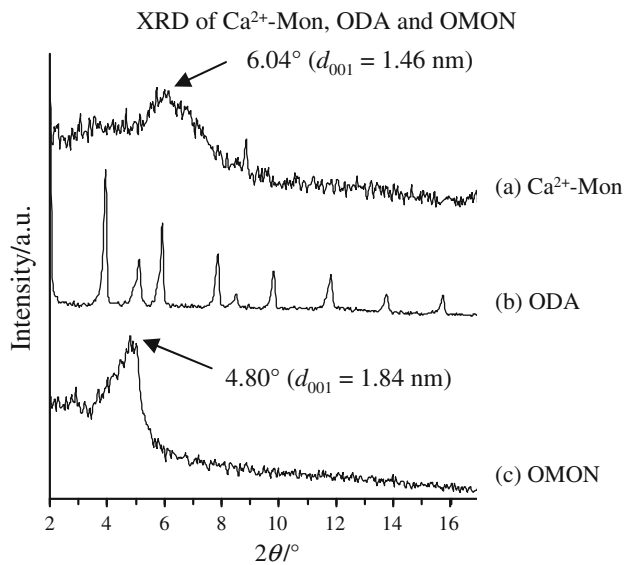


Fig. 1 (001) peak of Ca²⁺-Mon at $2\theta = 6.04^\circ$ (1.46 nm) in (a) is shifted to 4.80° (1.84 nm) in OMON (c) due to the intercalation of modifier cation from ODA (b)

where $P_e(T_p)$ = equilibrium polarization at polarizing temperature, τ_o = relaxation time at infinite temperature, E = activation energy, k = Boltzmann constant, h = heating rate

Results and discussion

XRD

Diffraction pattern in Fig. 1a shows the XRD scan on Ca²⁺-Mon clay. The characteristic peak at $2\theta = 6.04^\circ$ gives the basal spacing of (001) plane, $d_{001} = 1.46 \pm 0.01$ nm.

Fig. 2 TSC profile of Ca²⁺-Mon in (a) shows the ρ_{Mon} peak at $T_{\text{max}} = 75^\circ\text{C}$ analogous to the DSC endothermic peak in (b) with the $T_{\text{mMon}} = 58^\circ\text{C}$

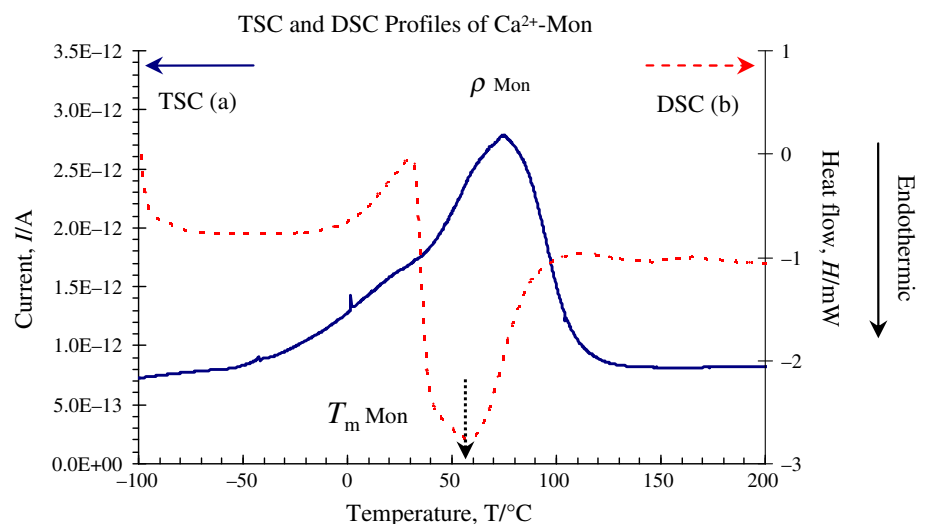


Figure 1b shows the diffraction pattern of ODA within $2\theta = 2^\circ$ – 16° . Sharp peaks demonstrate a number of crystalline structures in ODA molecular structure. Chemical modification on Ca²⁺-Mon into OMON involved the Ca²⁺ cation replacement with octadecylammonium (C₁₈H₃₇NH₃⁺) cation inside the layered clay gallery. As a result, the clay characteristic (001) peak is shifted to $2\theta = 4.80^\circ$ as shown in Fig. 1c, which gives the new basal spacing, $d_{001} = 1.84 \pm 0.01$ nm. The increase in d_{001} spacing of around 0.38 nm indicates the intercalations of the modifier cation, which had increased the OMON gallery height.

Comparison between DSC and TSC

Ca²⁺-Mon clay mineral

Figure 2a shows thermoelectrical profile from TSC measurement on Ca²⁺-Mon, while Fig. 3b shows DSC thermogram of the clay, where both are in low temperature range from -100 to 200°C . In Fig. 2b, an endothermic peak with melting point at $T_{\text{mMon}} = 58^\circ\text{C}$ covers a temperature of about 70°C . This peak indicates dehydration of interlayer water inside the Ca²⁺-Mon. According to Bray [14], dehydration process within 30 to 150°C causes the reduced in interplanar spacing of Ca²⁺-Mon. The dehydration in Ca²⁺-Mon caused the loss of interlayer water that distorts the water molecule structures as shown in the previous study [5].

Figure 2a shows a big relaxation peak with its maximum at $T_{\text{max}} = 75^\circ\text{C}$ falls within the endothermic temperature range. The peak is referred to as ρ_{Mon} peak and can be related to the relaxation of polarized water molecules in Ca²⁺-Mon and space charge released due to dehydration proses.

Fig. 3 ρ_{ODA} (55 °C) and $\rho_{1\text{ODA}}$ (76 °C) peaks in TSC profile (a) are analogous to the $T_{\text{m}1}$ (63 °C) and $T_{\text{m}2}$ (90 °C) peaks from DSC profile in (b), respectively. The first peak at 28 °C is assigned as the α_{ODA} peak and comparable to the T_{gODA} around 34 °C in the inset

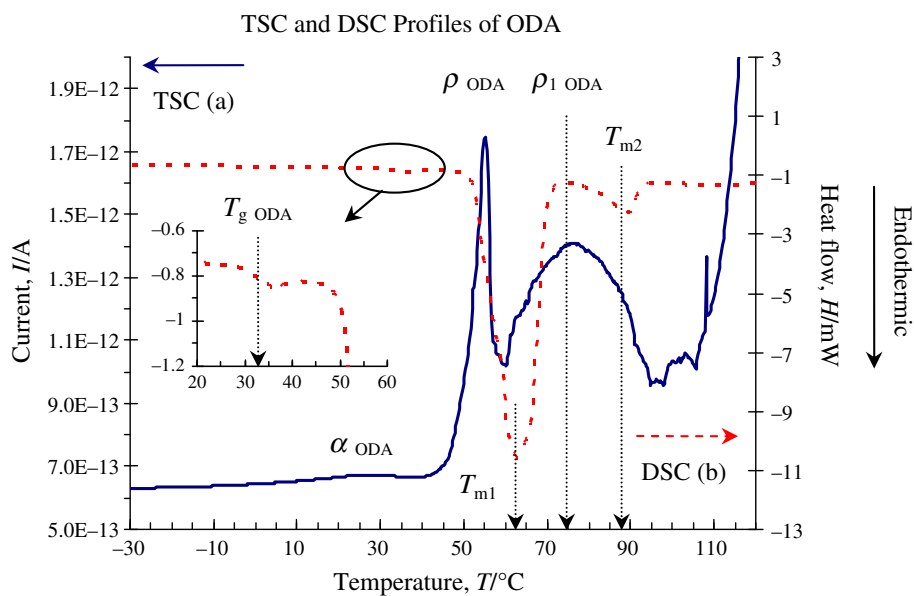
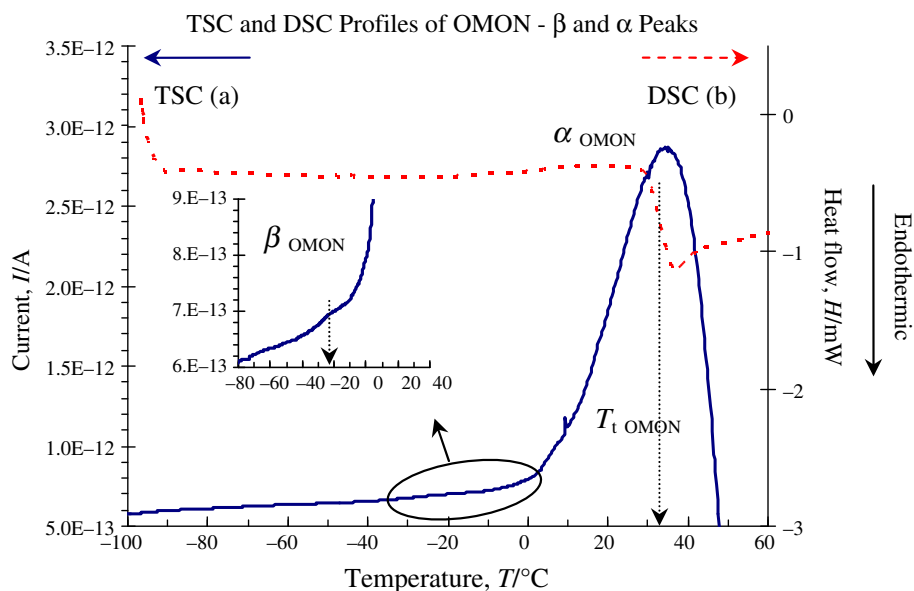


Fig. 4 A small hump at -23 °C in inset is assigned as the β_{OMON} peak. It appears before the α_{OMON} peak at 35 °C (a), which is analogous to the T_{t} at 33 °C in the DSC profile (b)



ODA

TSC measurement on ODA sample produced three relaxation peaks shown in Fig. 3a, which are analogous to a thermal transition and endothermics from DSC scan. The peaks with $T_{\text{max}} = 28, 56$ and 76 °C are assigned as $\alpha_{\text{ODA}}, \rho_{\text{ODA}}$ and $\rho_{1\text{ODA}}$, respectively. The α_{ODA} peak coincides with a thermal transition in Fig. 4b that gives the $T_{\text{gODA}} = 34$ °C. The peak indicates depolarization processes were induced by segmental motions of ODA chains during phase change around the T_{gODA} .

From Fig. 3a, the maximum of ρ peaks are within the temperature range of endothermic peaks, where $T_{\text{m}1} = 63$ °C and $T_{\text{m}2} = 90$ °C. Analysis shows that the

difference in the T_{max} of ρ peaks ($\nabla T_{\text{max}} = \sim 21$ °C) is comparable to the difference in T_{m} ($\nabla T_{\text{m}} = \sim 27$ °C) from the melting peaks in DSC profile. From Fig. 4b, temperature deviation between T_{m} and T_{g} about 29–56 °C can be related to chains motions in ODA crystallite structures. The methylene (CH_2) groups in ODA chains started to experience liquid-like motions at temperature 40 °C below the T_{m} [15]. The motions then led to the process of crystallite melting in the material. Therefore, the differences in the T_{max} of α and ρ peak about 27–47 °C show the effects of structural changes on TSC peaks. Pristine ODA structures were properly illustrated and described in the literature [11]. The trends were found similar, and it shows gradually disrupted during the melting process of crystallites. The

process not just induced relaxation of polarized molecules, but it also released space charges that generated the ρ_{ODA} and ρ_{1ODA} peaks.

OMON

TSC profile in Fig. 4a shows a small hump with its maximum at $T_{\text{max}} = -23\text{ }^{\circ}\text{C}$ is assigned as the β peak of OMON (β_{OMON}). The β_{OMON} peak demonstrates the effects of localized motions by the short-chain segments in ODA structure. In Fig. 5b, there is no significant thermal transition around the peak temperature (-40 to $-10\text{ }^{\circ}\text{C}$) that can be related to the phase change induced by cooperative motion of ODA chains. It thus suggests that the depolarization process behind the β_{OMON} peak involved only noncooperative localized motions of ODA chains as illustrated in Fig. 5. Further increase in temperature, T , generated a thermal transition at $T_{\text{gOMON}} = 33\text{ }^{\circ}\text{C}$.

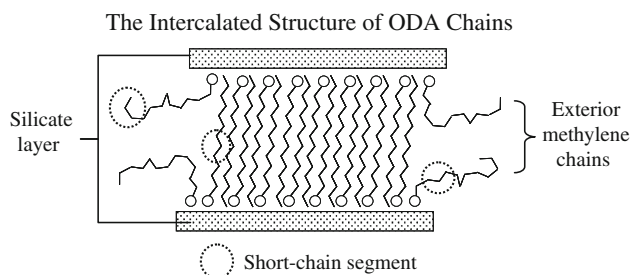
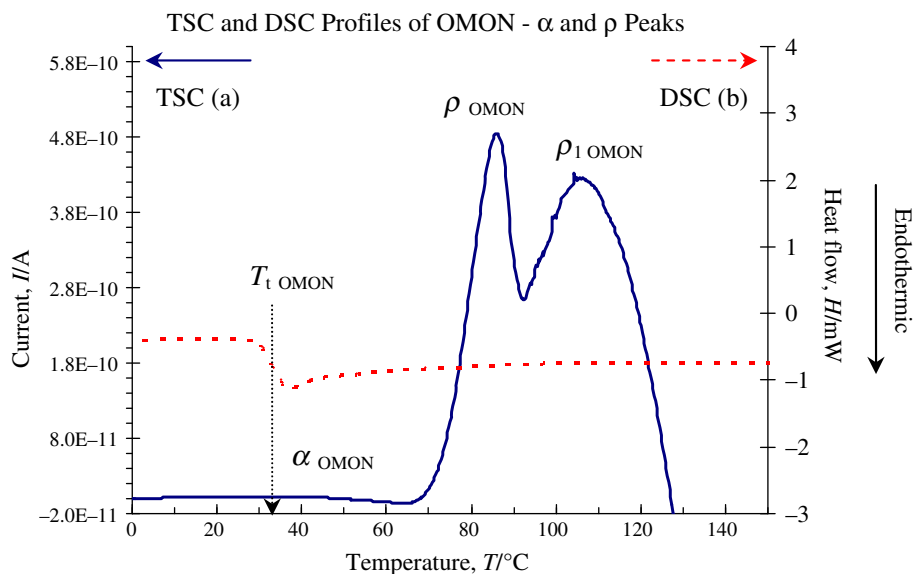


Fig. 5 Schematic diagram of the intercalated ODA cations shows the short-chain segments in methylene chains and the exterior chains which are free to coil and entangle with organic molecules. Printed with permission [11]

Fig. 6 ρ_{OMON} ($86\text{ }^{\circ}\text{C}$) and ρ_{1OMON} ($105\text{ }^{\circ}\text{C}$) peaks in (a) represent the changes of ODA structures in OMON that is absent in the DSC profile in (b)



Cooperative segmental motions of ODA chains around the T_{gOMON} produced the OMON α peak (α_{OMON}) in Fig. 5a, where its T_{max} is about $35\text{ }^{\circ}\text{C}$.

Figure 6a shows the relaxation peak of α_{OMON} , ρ_{OMON} ($T_{\text{max}} = 86\text{ }^{\circ}\text{C}$) and ρ_{1OMON} ($T_{\text{max}} = 105\text{ }^{\circ}\text{C}$) comparable to the α_{ODA} , ρ_{ODA} and ρ_{1ODA} peaks in Fig. 4a, respectively. These peaks of OMON indicate the presence of ODA chains in the modified Ca²⁺-Mon particles. The peaks maximum (T_{max}) in Table 1, however, is relatively higher than their counterparts for ODA. The increased T_{max} shows the effects of octadecylammonium cation intercalations inside the OMON gallery. The increments about 25–56% show relatively higher thermal energy was used by the intercalated ODA cations to induce dipoles and space charges relaxations. The presence of ODA chains in OMON, however, is hardly detected in the DSC profile in

Table 1 Temperature of DSC thermal transition and endothermic peaks and maximum temperature of TSC peaks in Ca²⁺-Mon, ODA and OMON

Sample	Technique	Temperature, $*T (T_{\text{max}})/^{\circ}\text{C} \pm 0.01$			
		(β)	$*T_{\text{g}} (\alpha)$	$*T_{\text{m1}} (\rho)$	$*T_{\text{m2}} (\rho_1)$
Ca ²⁺ -Mon	DSC	–	–	58, T_{mMON}	
	TSC	–	–	(75, ρ_{MON})	
ODA	DSC	–	34	63	90
	TSC	–	(28)	(55)	(76)
OMON	DSC	–	33	–	–
	TSC	(–23)	(35)	(86)	(105)

* DSC; ()—TSC

Fig. 6b. Table 1 lists only one thermal transition at $T_t = 33$ °C that can be related to ODA chains in OMON. It thus demonstrates the good sensitivity of TSC technique in detecting molecular motions in such confined space of the Ca^{2+} -Mon gallery.

Conclusions

TSC system used in this work is capable of demonstrating several relaxation effects as indicated by β , α and ρ peaks. Analysis shows that the peaks can be associated with thermal transition and melting processes observed in DSC curve. Despite the differences in TSC and DSC basic principles, both techniques measure the effects of molecular motions. Segmental motions by ODA main chains that caused the phase transition at $T_{i\text{OMON}} = 33$ °C also induced depolarization processes of α_{OMON} peak at $T_{\text{max}} = 35$ °C. Extensive molecular motions had led to molecular structure disruptions as shown by the DSC endothermics at $T_{\text{mMON}} (58$ °C), $T_{\text{mIODA}} (63$ °C) and $T_{\text{m2ODA}} (90$ °C). In TSC scan, these structural changes caused the release of space charges that curved the $\rho_{\text{MON}} (75$ °C), $\rho_{\text{ODA}} (55$ °C) and $\rho_{\text{IODA}} (76$ °C) peaks, respectively.

The appearance of β_{OMON} peak at $T_{\text{max}} = -23$ °C shows that TSC technique is capable of demonstrating the effect of localized short-chain motions at molecular level, an effect that cannot be identified using DSC technique. More evidences of the better sensitivity of TSC technique are shown by the $\rho_{\text{OMON}} (86$ °C) and $\rho_{\text{IOMON}} (105$ °C) peaks. They represent the effects of ODA chains motions in confined space of Ca^{2+} -Mon gallery. The effect that is absent in the DSC profile proves the intercalation of ODA cations into the OMON gallery. It is supported by the increased T_{max} of α (25%) and ρ (38–56%) peaks in OMON. TSC technique thus is a complimentary technique that adds more information on the effects of various thermally induced motions at molecular level. It is important to understand that both TSC and DSC techniques successfully measure the molecular motion, but one is originated by molecular motion by thermal effect and the other is originated by molecular motion due to DC field. It is also

important that TSC peak is also influenced by other parameters such as relaxation time, activation energy and charge released.

References

1. Theng BKG. Formation and properties of clay-polymer complexes. Amsterdam: Elsevier; 1979.
2. Li H, Sheng G, Teppen BJ, Johnston CT, Boyd SA. Sorption and desorption of pesticides by clay minerals and humic acid-clay complexes. *Soil Sci Soc Am J.* 2003;67:122–31.
3. Joshi GV, Kevadiya BD, Patel HA, Bajaj HC, Jasra RV. Montmorillonite as a drug delivery system: intercalation and in vitro release of timolol maleate. *Int J Pharm.* 2009;374:53–7.
4. Ganguly S, Dana K, Ghatak S. Thermogravimetric study of n-alkylammonium-intercalated montmorillonites of different cation exchange capacity. *J Therm Anal Calorim.* 2010;100(1):71–8.
5. Halim NA, Ibrahim ZA, Ahmad AB. Intercalation of water and guest molecules within Ca^{2+} -Montmorillonite: DSC studies in low temperature range. *J Therm Anal Calorim.* 2010;102:983–8.
6. Saw CK, Collins G, Mencil J, Jaffe M. Thermally induced reorganization in LCP fibers: molecular origin of mechanical strength. *J Therm Anal Calorim.* 2008;93(1):175–82.
7. Satoto R, Morikawa J, Hashimoto T. Effect of catalyst on thermally stimulated current in poly(ethylene terephthalate). *J Therm Anal Calorim.* 2002;70:713–22.
8. Vanderschueren J, Gasiot J. Field-induced thermally stimulated currents. In: Braunlich P, editor. Thermally stimulated relaxation in solid. Topics in applied physics, vol. 37. New York: Springer-Verlag; 1979. p. 135–223.
9. Prasad KR. Thermally stimulated relaxation and electrical conduction polyacrylamide. *Int J Sci Technol.* 2013;2(2):73–6.
10. Gaur MS, Singh PK, Ali A, Singh R. Thermally stimulated discharged current (TSDC) characteristic in β -phase PVDF-BaTiO₃ nanocomposites. *J Therm Anal Calorim.* 2014;17(3):1407–17.
11. Halim NA. Thermo-electrical and mechanical studies on polymer-organically modified montmorillonite composites. PhD Thesis. University Malaya, Kuala Lumpur; 2010.
12. Rich CI, Kunze GW. Soil clay mineralogy (a symposium). North Carolina: Uni. Carolina Press; 1964.
13. Turnhout JV. Thermally stimulated discharge of electrets. In: Sessler GM, editor. Topics in applied physics—electrets. New York: Springer-Verlag; 1980.
14. Bray HJ, Redfern SAT, Clark SM. The kinetic of dehydration in Ca-montmorillonite: an in situ X-ray diffraction study. *Mineral Mag.* 1998;62(5):647–56.
15. Wunderlich B. Thermal properties of aliphatic nylons and their link to crystal structure and molecular motion. *J Therm Anal Calorim.* 2008;93(1):7–17.